EPJ Web of Conferences **87**, 04011 (2015)
DOI: 10.1051/epjconf/20158704011

Development of a Millimeter-Wave Beam Position and Profile Monitor for Transmission Efficiency Improvement in an ECRH System

T. Shimozuma[1], S. Kobayashi[1], S. Ito[1], Y. Ito[1], S. Kubo[1], Y. Yoshimura[1], M. Nishiura[2], H. Igami[1], H. Takahashi[1], Y. Mizuno[1], K. Okada[1], and T. Mutoh[1]

[1] *National Institute for Fusion Science, Toki-city, 509-5292, Japan*
[2] *Graduate School of Frontier Science, the University of Tokyo, Chiba-city, 277-8561, Japan*

Abstract. In a high power Electron Cyclotron Resonance Heating (ECRH) system, a long-distance and low-loss transmission system is required to realize effective heating of nuclear fusion-relevant plasmas. A millimeter-wave beam position and profile monitor, which can be used in a high-power, evacuated, and cooled transmission line, is proposed, designed, manufactured, and tested. The beam monitor consists of a reflector, Peltier-device array and a heat-sink. It was tested using simulated electric heater power or gyrotron output power. The data obtained from the monitor were well agreed with the heat source position and profile. The methods of data analysis and mode-content analysis of a propagating millimeter-wave in the corrugated waveguide are proposed.

1 Introduction

In a high power Electron Cyclotron Resonance Heating (ECRH) system with long-distance transmission lines, the reliable millimeter-wave (mmw) transmission can be much improved by evacuation, sufficient cooling, and precise alignment of the whole transmission system. For example, in the Large Helical Device (LHD) of National Institute for Fusion Science (NIFS), the length of the ECRH transmission line, which consists of corrugated waveguides, miterbends, and some mmw components, extends over 100 meters from gyrotrons to antennas [1, 2]. A schematic view of the recent ECRH system in LHD is illustrated in Fig. 1. The gyrotron system consists of three 1-1.5 MW / 77 GHz, one 1 MW / 154 GHz, one 0.45 MW / 82.7 GHz, and one 0.2 MW Continuous Wave (CW) / 84 GHz gyrotrons.

In order to maintain high transmission efficiency, the method of precise mmw beam alignment is required. Alignment methods of the corrugated waveguides and methods of a propagating mode-content analysis in the waveguide have been proposed and developed[3–6]. These methods were based on the measured field pattern on the target plate irradiated from an open edge of the corrugated waveguide. The mode-content could be analyzed using the phase retrieval method and mode decomposition by some eigen modes in the corrugated waveguide. Such measurement consequently had to be performed in the atmosphere at several positions in the transmission line using lower power and short pulse irradiation. As a real-time mode analyzer, a 5-port miterbend directional coupler for mode analysis was developed and tested in the corrugated waveguide [7, 8]. However, mismatch between the mmw axis and the waveguide axis possibly occurs during high power and CW operation. A real-time mmw beam-position and profile monitor (BPM) is required to evaluate the position and profile of a high power (Megawatt level) mmw even in the evacuated corrugated waveguide. We proposed a new type of BPM which can be used in the evacuated corrugated waveguide in real-time [9, 10].

In this paper, we report the idea, design, manufacturing, and initial test results of the new-type propagating mmw beam position and profile monitor. The method of analyzing the propagating mode contents in the corrugated waveguide is also proposed. In Sec. 2, a basic idea of the in-situ millimeter-wave beam position and profile monitor is briefly explained. In Sec. 3, high power test results using low spatial resolution BPM will be described. Design, manufacturing, and test results of the BPM with higher spatial resolution (52 Peltier devices) will be given in Sec. 4. One possible method of the mode-content analysis using BPM data will be proposed in Sec. 5. Finally, Section 6 will be devoted to the summary.

2 Basic Idea of an in-situ Millimeter-Wave Beam Position and Profile Monitor (BPM)

The idea of the BPM proposed is as follows. A two-dimensional array of Peltier devices is aligned and installed on the atmospheric side of a thin miterbend reflector with a heat-sink, as shown in Fig. 2. An mmw beam propagating in the corrugated waveguide is reflected on the mirror surface of the miterbend and partly absorbed in the reflector plate. The generated heat by Ohmic loss of

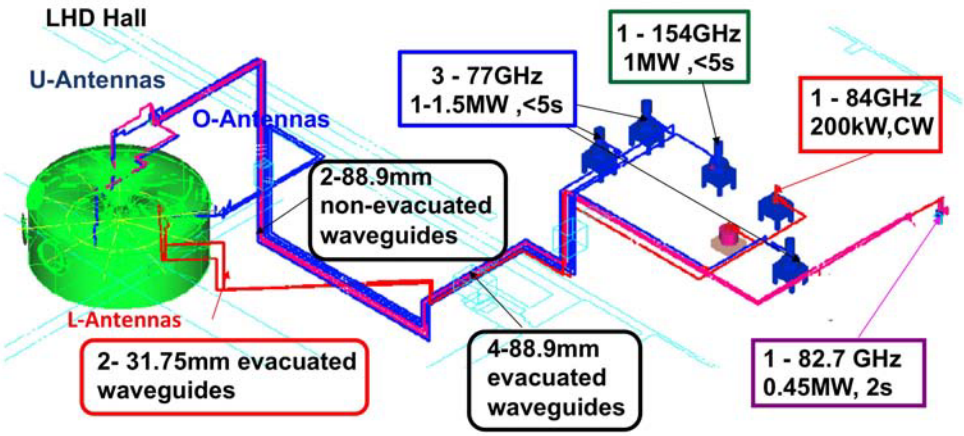

Figure 1. Recent (FY2013) ECRH system in LHD. Gyrotrons, transmission line, and antenna system.

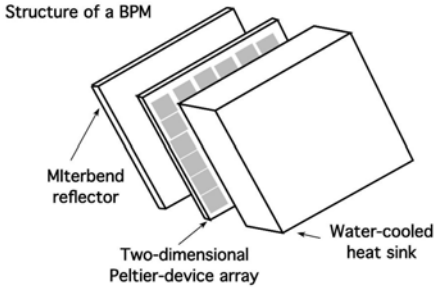

Figure 2. Structure of a beam position and profile monitor (BPM) installed in the miterbend reflector. The BPM consists of a reflector, Petier Device array and heat-sink.

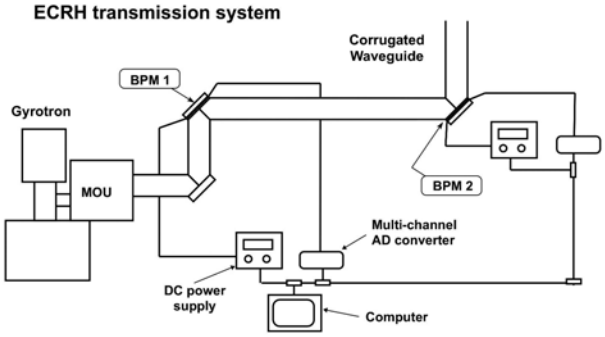

Figure 3. Schematic view of a BPM system to analyze the mode-content of propagating waves in the transmission line. The Peltier device array in two BPMs is operated by DC power supplies controlled by PC and voltage data of the devices are acquired by A/D convertors which are also controlled by PC through the network.

the electromagnetic wave diffuses to the outside of the reflector and is removed by the Peltier devices. The voltage of each Peltier device is approximately expressed as the following equation.

$$V = IR + S(T_H - T_C) \tag{1}$$

where I, R, and S are electric current, resistance, and Seebeck coefficient of the Peltier device, respectively. T_H and T_C represent hot-side (heat-sink side) and cold-side (reflector side) temperature of the Peltier device.

When these devices are connected serially and driven by the constant current control (I = constant), the voltage change of each device is almost linearly proportional to the temperature change of the cold-side of the device, if the temperature at the hot-side of the Peltier device is kept constant. The information of the two-dimensional temperature profile of the miterbend reflector can give the real-time information of the position and profile of the mmw beam. If two BPMs are installed apart from about one beat wavelength of the $HE_{11}(LP_{01})$ main mode and the $HE_{21}(LP_{11})$ lowest converted mode in the transmission line, mode contents included could be determined from two beam profile information. The whole system of the BPM to analyze the mode content of the propagating wave in the corrugated waveguide is illustrated in Fig. 3.

3 A Test BPM Module and High Power Test Results

A prototype equipment, which consists of a copper reflector with 1mm thickness, a two-dimentional array of eighteen Peltier devices (one device size is 20 mm square), a fin-type heat-sink, a power supply, A/D convertors, and a control PC, was constructed and tested. At the beginning, this equipment was tested using a circular electric heater with 45 mm in diameter (heating power was about 14 W) attached on the reflector plate. The heated positions could be well distinguished. Then, the equipment was installed in one of the miterbends in the LHD transmission line, which is connected to an 82.7 GHz gyrotron. Another side of the miterbend was connected to a dummy load. The system for testing is shown in Fig. 4.

High power test was performed using 82.7 GHz power with approximately 200 kW output and 100 ms pulse every 30 s. The temperature increase of the reflector measured directly by an RTD was about 0.5 degree around the center. Figure 5 a) shows a pattern of the voltage change

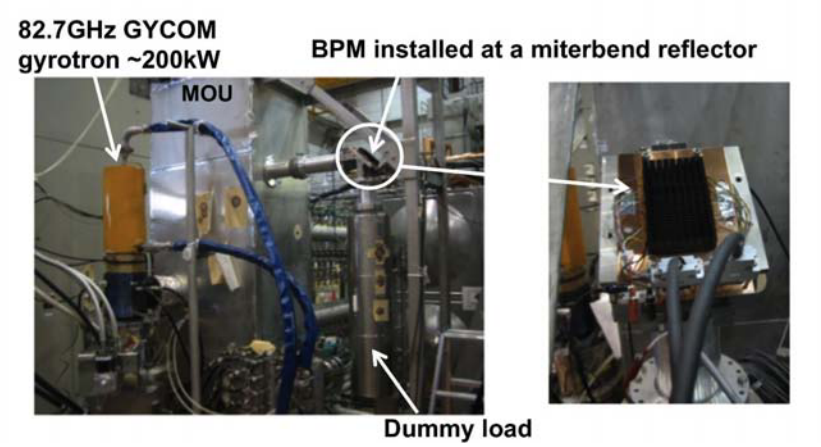

Figure 4. High power test configuration using gyrotron output. BPM was installed at the miterbend just in front of the water dummy load. The BPM has a cooling fin on the hot-side of the BPM.

normalized by the initial voltage of each Peltier device. Each quadrate in the figure corresponds to the device position. The ellipse indicated by a white dashed-line corresponds to the cross section of the corrugated waveguide at the miterbend. In this case, the peak of the voltage change is slightly off-center. After the test, the BPM was replaced by an absorber-coated reflector and a trial to obtain a thermal image was performed using an IR camera at the same position. Figure 5 b) shows the obtained temperature profile. The position attained peak temperature well coincides with the position of the highest voltage change shown in Fig. 5 a).

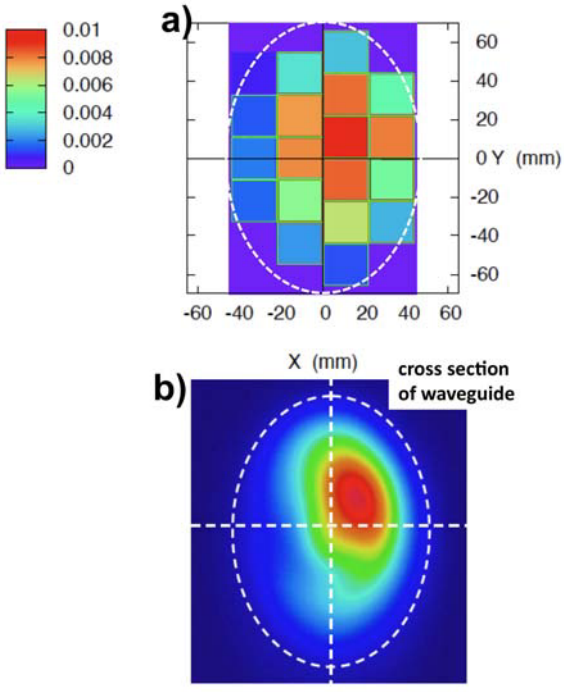

Figure 5. Pattern of the temperature increase of the reflector. a) Pattern obtained by BPM. b) Infrared image on a reflector coated by mmw absorber.

4 Fabrication of a High Spatial Resolution BPM Module and Test Results Using a Simulated Heat Source

A higher spatial resolution BPM, which consisted of 52 Peltier devices, was developed for high power mmw transmission. A diameter of the corrugated waveguide is 88.9 mm. Each Pelter device has a 10.3 mm square dimension and its thickness is 3.8 mm. The Peltier devices are aligned on a double-sided printed wiring board because many wirings are required. This is shown in Fig. 6 top figure. In order to conduct several hundreds kilo Watt CW transmission, a water-cooled copper heat-sink was adopted to handle the Ohmic loss of several hundred Watt CW power on the miterbend reflector, shown in Fig. 6 bottom figure. The material of the miterbend reflector is a pressure welded copper and stainless-steel board. The stainless-steel part was machined to insert the circuit board of the Peltier device array. The thickness of the copper reflector is 3 mm to withstand atmospheric pressure for the evacuated corrugated waveguide.

Initially we tested the BPM using a circular heater with 45 mm in diameter as a heat source. It was set around the center of the miterbend mirror surface. The procedure of the experiment was as follows. At first, the current of serially connected Peltier devices was turned on at $t = 0$ and the reflector side was cooled down. Then the heater was turned on from $t = 33$ s to 43 s as shown in Fig. 7 a) and c) (green curves). Figures 7 a) and c) also show waveforms of the raw voltage signals of each Peltier device which locates around the center (U30) in a) and the edge (U01) in c) of the BPM, respectively. The sampling time is 1 ms. Because the temperature difference between cold and hot sides of the Peltier device decreases during the heater-on, the voltage of the device decreases, as is suggested in Eq. (1). Probably, it will saturate in the steady-state. Because the raw voltage signals are rather noisy, those signals are averaged and plotted as red curves in Fig. 7 b) and d), respectively.

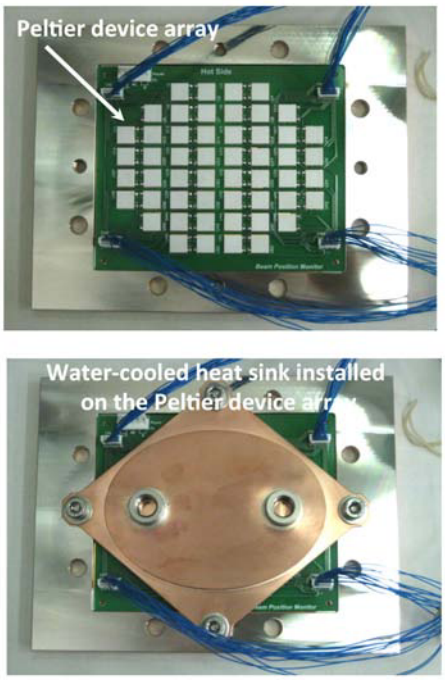

Figure 6. High spatial resolution BPM. Top: Peltier devices, which are aligned on a double-sided printed wiring board, are installed on the atmospheric side of the reflector . Bottom: Reflector and Peltier device array with a copper heat-sink

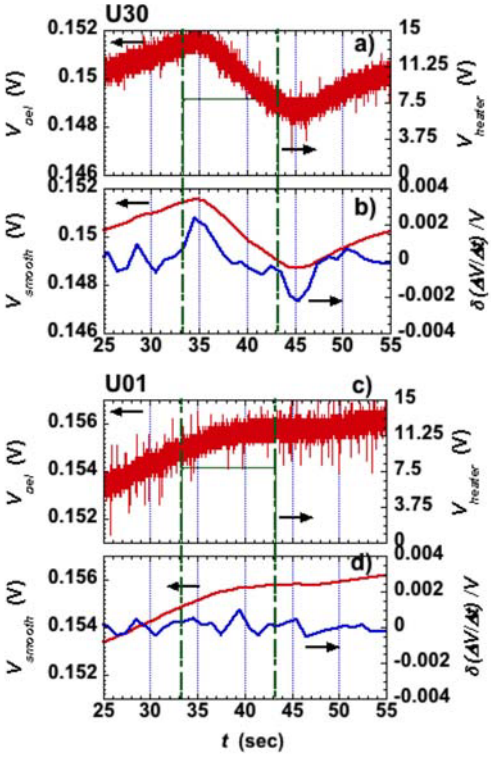

Figure 7. Time evolution of Peltier device voltage (red) in a) for U30 device and in c) for U01 device. Heater voltage (green) is also plotted. In b) and d), time averaged Peltier device voltage V_{smooth} (red) and $S = \delta(\Delta V_{\mathrm{smooth}}/\Delta t)/V_{\mathrm{smooth}}$ (blue) are plotted.

We attempted a transient analysis of the variation of the Peltier device voltage. In order to find the start timing of the voltage decrease, the smoothed voltage signals are linearly fitted partly, and the difference of their gradients, $S = \delta(\Delta V_{\mathrm{smooth}}/\Delta t)/V_{\mathrm{smooth}}$, is calculated and shown as blue curves in Fig. 7 b) and d). At the earliest timing when the values S for all Peltier devices becomes maximum after heater-on timing, the values S of all Peltier devices were mapped in Fig. 8. The area with large S value well coincides with the heater position indicated by a black dashed-line circle. The method of the analysis, however, should be improved considering the heat conduction in the copper reflector plate.

The algorithm to determine the temperature change from the voltage change of each Peltier device was considered and confirmed experimentally. Additionally, a method of the mode content analysis using the obtained data is considered and proposed in the next section.

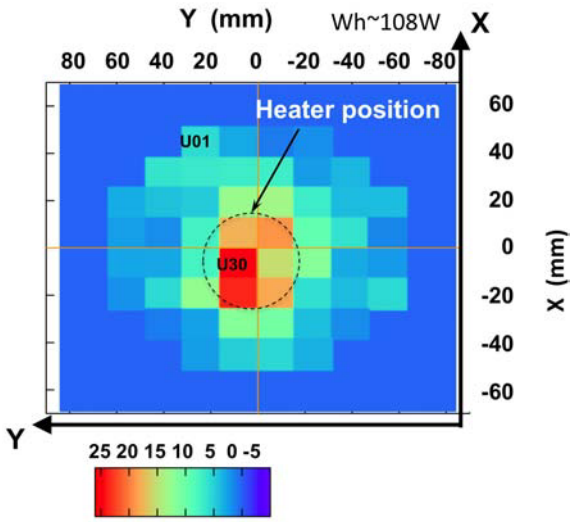

Figure 8. The values of $S(t = 34.5s) = \delta(\Delta V_{\mathrm{smooth}}/\Delta t)/V_{\mathrm{smooth}}$ are mapped on the each Peltier device position. The black dashed-line circle indicates the heater position attached.

5 Method of Mode Content Analysis

Using the signals obtained by the BPM, a method of mode content analysis is considered according to the method proposed in the reference [11]. For simplicity, linear polarized modes in a circular corrugated waveguide [12] are considered, which are expressed as the following equations:

$$\mathrm{LP}^{\mathrm{y}}_{\mathrm{nm}}(\mathrm{e}) : \boldsymbol{E}_{\perp}(r,\theta) = \hat{y}\,\sqrt{2} f_{\sigma} J_n(X_{\sigma}\cdot r/a)\cos(n\theta) \quad (2)$$

$$\mathrm{LP}^{\mathrm{y}}_{\mathrm{nm}}(\mathrm{o}) : \boldsymbol{E}_{\perp}(r,\theta) = \hat{y}\,\sqrt{2} f_{\sigma} J_n(X_{\sigma}\cdot r/a)\sin(n\theta) \quad (3)$$

$$\mathrm{LP}^{\mathrm{x}}_{\mathrm{nm}}(\mathrm{e}) : \boldsymbol{E}_{\perp}(r,\theta) = \hat{x}\,\sqrt{2} f_{\sigma} J_n(X_{\sigma}\cdot r/a)\cos(n\theta) \quad (4)$$

$$\mathrm{LP}^{\mathrm{x}}_{\mathrm{nm}}(\mathrm{o}) : \boldsymbol{E}_{\perp}(r,\theta) = \hat{x}\,\sqrt{2} f_{\sigma} J_n(X_{\sigma}\cdot r/a)\sin(n\theta), \quad (5)$$

where n, m are mode numbers and X_σ is the eigen value of the mode σ with (n, m). a expresses the radius of the waveguide and the normalization constant f_σ is

$$f_\sigma = \frac{Z_0}{a\sqrt{\pi}J_{n+1)}(X_\sigma)} = -\frac{Z_0}{a\sqrt{\pi}J_{n-1)}(X_\sigma)}. \quad (6)$$

The magnetic field for each mode is expressed as

$$\boldsymbol{H}_\perp = (-\hat{x}E_y + \hat{y}E_x)/Z_0, \quad (7)$$

where Z_0 is a characteristic impedance. Electric field profiles of typical lower order LP_{nm} modes are graphically plotted in Fig. 9. The direction of the electric field is oriented to Y-direction.

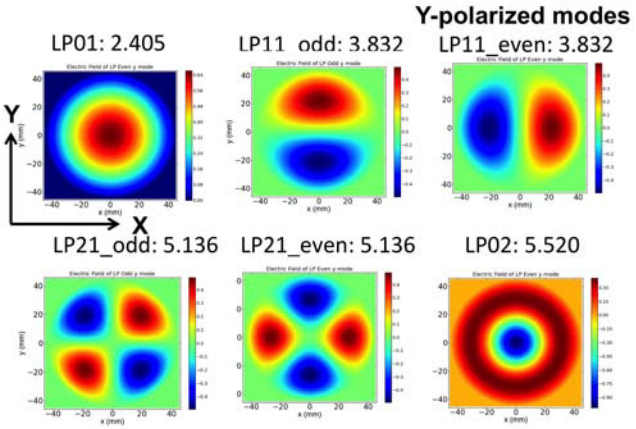

Figure 9. Electric field profile of typical lower-order LP_{nm} modes. For each mode, "*even*" or "*odd*" and eigen value X_σ are indicated in the figure.

Generally, a propagating mmw in the corrugated waveguide is expressed as a superposition of several eigen modes σ $(= 0 \cdots N)$. The electric field at the position of $(x_i, y_j.z_k)$ is described by the following equation:

$$\boldsymbol{e}_{tot}(x_i, y_j, z_k) = \sum_{\sigma=0}^{N} \sqrt{p_\sigma} \exp\{j(\phi_\sigma - k_\sigma z_k)\}\boldsymbol{E}_\sigma(x_i, y_j) \quad (8)$$

$$x_i = i \times \Delta x \quad (9)$$

$$y_j = j \times \Delta y, \quad (10)$$

where $i, j = 0 \cdots M-1$, and p_σ, ϕ_σ, and k_σ are the power, phase, and wave-number of the propagating mode σ, respectively. The evaluation function W_{tot} for determining mode content is defined by the summation of square value of the difference between the measured O and theoretical T functions,

$$W_{tot}(p_\sigma, \phi_\sigma) = \sum_{k=0}^{n-1} W(z_k), \quad (11)$$

where

$$W(z_k) = \sum_{i=0}^{M-1}\sum_{j=0}^{M-1}\{O(x_i, y_j, z_k) - T(x_i, y_j, z_k)\}^2 \quad (12)$$

$$T(x_i, y_j, z_k) = \frac{|\boldsymbol{e}_{tot}(x_i, y_j, z_k)|^2}{|\boldsymbol{e}_{tot}|^2_{MAX}} \quad (13)$$

When the mode with $\sigma = 0$ is assumed to be the LP_{01} fundamental mode with the phase $\phi_0 = 0$ and $\sum_{\sigma=0}^{N} p_\sigma = 1$, each p_σ, ϕ_σ can give the ratio of mode-content and the initial phase of each mode σ.

6 Summary

In the recent ECRH system of LHD, three Mega-Watt 77 GHz and one 154 GHz gyrotrons have been developed and installed under collaboration with University of Tsukuba and JAEA. In total, 4.6 MW power was injected into LHD using these gyrotrons in the 2013 LHD experimental campaign.

In order to transmit a Mega-Watt millimeter-wave (mmw) with the low-loss fundamental mode of HE_{11} or LP_{01} in the long-distance corrugated waveguide with high reliability, precise alignment of the mmw to the waveguide axis and matching of a beam waist size and the phase profile at the waveguide entrance are required. The development of an mmw beam position and profile monitor (BPM) and propagating mode-content analyzer are strongly desired. We proposed such an mmw BPM which can be installed even in an evacuated high-power CW transmission lime. The monitor consists of a two-dimensional Peltier-device array installed on the atmospheric side of a miter-bend mirror and a heat-sink. BPMs with both 18 and 52 Peltier device arrays were manufactured and tested using simulated heater power or mmw power from a gyrotron. The measured voltage of each Peltier device well reflected the input heat profile. A method of mode-content analysis using these data is also proposed.

Acknowledgements

This work is supported by National Institute for Fusion Science under grant ULRR701 and is also supported by a grant for scientific research from the Ministry of Education, Science and Culture of Japan (21560058, 24560066).

References

[1] T. Shimozuma, S. Kubo, Y. Yoshimura, et al., "Handling Technology of Mega-Watt Millimeter-Waves for Optimized Heating of Fusion Plasmas" Journal of Microwave Power & Electromagnetic Energy **43**, 60 (2009).

[2] T. Shimozuma, H. Takahashi, S. Kubo, Y. Yoshimura, H. Igami, et al., "ECRH-Related Technologies for High-Power and Steady-State Operation in LHD", Fusion Science and Technology, **58**, 530 (2010).

[3] T. Shimozuma, H. Idei, M.A. Shapiro, R.J. Temkin, et al., "Alignment Method of ECH Transmission Lines Based on the Moment and Phase Retrieval Method Using IR Images" J. Plasma Fusion Res. **81**, 191 (2005).

[4] T. Shimozuma, H. Idei, M.A. Shapiro, R.J. Temkin, et al., "Mode-Content Analysis and Field Reconstruction

of Propagating Waves in Corrugated Waveguides of an ECH System", Plasma and Fusion Research **5**, S1029 (2010), DOI: 10.1585/pfr.5.S1029

[5] H. Idei, M.A. Shapiro, R.J. Temkin, T. Shimozuma, and S. Kubo, "Mode Retrieval from Intensity Profile Measurements Using Irradiant Waveguide-Modes", 34th International Conference on Infrared, Millimeter, and Terahertz Waves, 2009. IRMMW-THz 2009, 21-25 Sept. 2009.

[6] Y. Oda, K. Kajiwara, K. Takahashi, A. Kasugai, M.A. Shapiro, R. J. Temkin, and K. Sakamoto, "Measurement of RF Transmission Mode in ITER Relevant EC H&CD Transmission Line", J Infrared Milli Terahz Waves **31**, 949 (2010), DOI 10.1007/s10762-010-9666-4.

[7] B. Plaum, W. Kasparek, C. Lechte, J. Ruiz, D. Tretiak, and H. Idei, "In-Situ Characterization of Spurious Modes in HE11 Transmission Lines with a 5-Port Coupler", EPJ Web of Conferences 32, 04010 (2012), DOI: 10.1051/epjconf/20123204010

[8] J. Ruiz, W. Kasparek, C. Lechte, B. Plaum, and H. Idei, "Numerical and experimental investigation of a 5-port mitre-bend directional coupler for mode analysis in corrugated waveguides", Infrared Milli Terahz Waves **33**, 491 (2012), DOI 10.1007/s10762-012-9883-0

[9] T. Shimozuma, H. Takahashi, S. Ito, et al., "Optimization of High Power and High Efficiency Operation of 77GHz Gyrotrons for ECRH in the Large Helical Device", Proceedings on 36th International Conference on Infrared, Millimeter, and Terahertz Waves, 2011, Houston, TX, USA W2A-1.

[10] T. Shimozuma, S. Kobayashi, S. Ito, et al., "Development of a Millimeter-Wave Beam Profile Monitor in Mega-Watt CW ECH Transmission Line", Plasma Conference 2011, Nov. 22-25, Kanazawa, Japan, 22P146-P.

[11] K. Ohkubo, S. Kubo, T. Shimozuma, Y. Yoshimura, H. Igami, and S. Kobayashi, "Mode Content Anlysis for ECH Transmission Lines by Burn Pattern and Nonlinear Optimization", Fusion Science and Technology **62**, 389 (2012)

[12] E.J. Kowalski, D.S. Tax, M.A. Shapiro, J.R. Sirigiri, R.J. Temkin, T.S. Bigelow, and D.A. Rasmussen, "Linearly Polarized Modes of a Corrugated Metallic Waveguide", IEEE Trans. on Microwave Theory and Techniques, **58**, 2772 (2010).